Magnetic Field Sensors for EM Geophysics

James Macnae[1] and Lachlan Hennessy.[1]

1. RMIT University, Melbourne, Australia

ABSTRACT

Of the 20 or more magnetic effects that have been used for measurement of magnetic fields, sensors based on the Faraday and Josephson effects have proven to be the best for electromagnetic surveys. To be useful, a sensor must have low internal noise and high sensitivity, as well as being linear and capable of operating unscreened in the earth's magnetic field. For sensors with noise levels less than 0.1 pT/√Hz in the EM bandwidth, atmospheric and rotation noise rather than internal noise is usually the limiting factor. SQUID sensors based on various superconducting effects have the lowest noise, but in practice are constrained by a range of factors including slew-rate and saturation issues, as well as the need for cryogenic fluids. All three sensors based on induction, voltage-sensed coils, current-sensed and feedback magnetometers achieve very low noise levels, provided that their effective area is large and their resistance low, requiring sufficient area and weight of typically Cu or Al wire. Several of the contributors to internal noise in an induction sensor are the same: thermal noise of the coil wire resistance, operational amplifier voltage and current noise. Induction coils, as voltage sensors, require damping to prevent oscillation, and the damping resistor is the dominant source of noise in the centre of the sensor bandwidth making these dB/dt sensors the noisiest of the three options for the same sensor weight. Voltage sensors are also subject to Barkhausen noise from any ferromagnetic core. Feedback and current sensing layouts, however, are not as sensitive to Barkhausen noise, do not need a damping resistor for stability, and so intrinsically have lower magnetic field noise than coil voltage sensors. Feedback sensors have similar noise levels to current sensors at low frequencies, but like voltage sensors, have increased noise at high frequency when compared to current sensors. In the field, natural noise and the limitations of 24 bit sensors in handling large fields near transmitters mean that the data acquisition system and its gains are controlling factors far more important than internal noise from SQUID, induction magnetometer or other highly sensitive sensors.

INTRODUCTION

There is a large variety in the physical effects of magnetism that can be measured, with over 20 fundamentally different methods of magnetic field measurement having proven useful in measurement applications. These magnetometers can have very different characteristics, and as such be suited to differing applications such as traffic detection, biomagnetics, proximity sensors, automotive, space weather, palaeomagnetics and exploration geophysics. A recent summary of some of these magnetometers is provided in Grosz et al. (2017).

This paper will discuss magnetic measurement of alternating electromagnetic (EM) fields in terrestrial geophysical applications. Several characteristics may distinguish sensors of an EM field that measure its magnetic component B or its time derivative dB/dt. In roughly decreasing order of importance from an EM perspective, desirable factors are listed in Table 1.

Of critical importance is that a geophysical EM sensor must operate in the earth's magnetic field and in the field cannot be located in a shielded chamber. Shielded chambers are of course routinely used for medical Magnetic Resonance Imaging and for palaeomagnetic rock measurements where the target can be located inside the shield. The useful geophysical sensitivity for static magnetic fields is often considered to be a fraction of a nanoTesla, significantly less than the typical diurnal and ongoing annual variation in the Earth's field. For EM on the other hand, the "noisiest" useful sensors in operation have sensitivity less than 10 pT/√Hz, with good sensors better than 0.1 pT/√Hz. In the field, there are many external noise sources (e.g. sferics, microphonics, cultural, transmitter waveform drift). This generally means that achieved survey noise levels in controlled source applications are determined more by the environmental noise rather than the sensor internal noise, particularly if this sensor internal noise is less than 0.1 pT/√Hz.

Different sensors have different bandwidths, and an ideal EM sensor needs to cover the range from less than 1 Hz to say 50 kHz. Limited geophysical surveys are conducted using VLF and radiowave sensors, but these will not be discussed here. Above 10 MHz, ground penetrating radar (GPR) is a useful technique where electric rather than magnetic sensors are optimum.

All good sensors are linear, as geophysically we usually need to separate "secondary" from "primary" and "noise" fields, a process requiring linearity. Small deviations from linearity such as slew-rate problems can be handled in processing, but are not desirable features of a sensor.

A step down in importance from the first four criteria is gradient tolerance which is occasionally critical if the sensor is to operate close to culture (e.g. pipes, fences, vehicles, transmitters or aircraft). This is mostly an issue for optical vapour and other resonance magnetometers, as all the sensor gas chamber needs to

be in the same magnetic field to resonate at the same measurable frequency.

Different sensors can be sensitive to total field or to a component of the field. Vectorial sensors are strongly affected by rotation in the earth's field, while scalar (total field) sensors only measure small secondary components that are in the direction of the much larger earth's field. A total field magnetometer used as an EM sensor will measure the horizontal magnetic North component at the magnetic equator (e.g. in India) but the vertical component near the poles.

Number / Importance	Desirable Characteristic	Notes
1	Must operate in the Earth's Field	Some otherwise "superb" sounding sensors with sub fT sensitivity sound great, but only work in low fields (magnetically shielded environments). Published papers do not always disclose this critical piece of information.
2	Sensitivity	Require noise level << 10 pT/√Hz, preferably < 0.1 pT /√Hz to be a useful / good sensor in practice.
3	Bandwidth	Need to be wideband for TEM, with good response from chosen base frequency (a variable, commonly 1 to 30 Hz) for several decades. High cut-off usually limited by unwanted noise considerations but need not be a sensor feature.
4	Linearity	All sensors saturate or have slew-rate limitations at some point, exploration often requires separation of small secondary fields form larger primaries
5	Gradient Tolerance	Will the sensor work in a strong field gradient?
6	Preferably Vector / unless Scalar required for rotation tolerance	Vector sensors need orientation. Scalar sensors measure vertical component at the magnetic poles and the horizontal magnetic north component at the magnetic equator.
7	Ease of use / reliability	Fast settling times, low and slow calibration drift, no need for cryogenics, minimum mass, bulk & insensitive to EM interference from e.g. mobile phones.
8	Inexpensive	Compared to other survey costs, usually not an issue.

Table 1: Desirable EM sensor characteristics

Practical considerations determine the economics of survey operation. An ideal sensor would have in addition to the essential characteristics; fast settling times, small calibration drifts (due to temperature variations and ageing); being light-weight, robust, not requiring cryogenic fluids, not being sensitive to out-of-bandwidth noise, and being available and inexpensive. System designers and field operators need in practice to consider the trade-offs between desirable and achievable hardware and operating procedures.

Nominal Sensitivity in range 1 to 10 Hz	**Technology**	**Notes**	**ITAR/DECO limit below which regulated**
10 nT/√Hz	MEMS	Miniature	
1 nT/√Hz	Nitrogen Vacancy	Fibre-Optic arrays	Fibre Optic 1 nT
	Cavity - Optomechanical		
100 pT/√Hz	100 m^2 multiturn Coil; Hall Effect; Magnetoelectric	Unamplified coil	
			Optical 20 pT
10 pT/√Hz	GMImpedance, GMResistance		Fluxgate 10 pT
	Commercial Fluxgates	Rugged and reliable	
1 pT/√Hz	100 m square loop; CNV	Cryogenic Nitrogen Vacancy	
	Inductive Magnetometer (air core),		
100 fT/√Hz			Induction Magnetometer 100 fT
	Inductive magnetometer (ferromagnetic core), Magnetoelectric 77°K HT SQUID 77°K	All SQUIDS in field without a remote reference have this noise level	SQUID 50 fT
10 fT/√Hz		No field benefits unless simultaneous remote referencing data acquired	
	LT SQUID 4.2°K		
1 fT/√Hz	SERF (low field)		

Table 2: Some typical quoted sensitivities in the 1 to 10 Hz range. Some high-sensitivity sensors of perceived military value are regulated by various Defence authorities such as ITAR (USA) and DECO (Australia). Many sensors have variants of lower noise than quoted here, e.g. sub 1 pT/√Hz fluxgates of small bandwidth (Bazinet et al., 2014) and sub 1 fT/√Hz LT SQUIDS (Storm et al., 2017). References for all other sensor types can be found in Table 3.

Table 2 presents a list of some common magnetic field sensor technologies, ranked in decreasing order of sensitivity, together with notes on the sensitivity level below which there are export restrictions set by governments based on military considerations. The use and export of controlled sensors is restricted by e.g. the Australian Defence Export Controls (DECO) act or the US International Traffic in Arms Trade Regulations (ITAR).

Useful Magnetic Effects and Applications

A list of 20 useful magnetic effects and their approximate date of publication is provided in Table 3. Only 4 effects meet the fundamental requirements of operating in the earth's ambient field and being sufficiently sensitive for EM, shown in Table 2. These are the currently used Faraday (induction coil) and Josephson (SQUID) effects. Not in commercial use are cryogenic magnetoelectric sensors and the recently described multipass cell atomic magnetometer. This last magnetometer is band-limited so not of immediate interest. Fluxgates and optical pumping magnetometers come close, but are significantly noisier than coils/SQUIDS in the EM bandwidth.

Magnetic Effect	Time-line	Usual Application	Geophysical Sensor Use	Problem with	Reference
Faraday	**1831**	**Induction coils and induction magnetometers**	EM, geophones	7(drift)	Dehmel (1989)
Magnetostriction	1842	Piezometers		2, 3, 4	Bichurin et al. (2017)
ΔE (Young's modulus)	1846	Acoustics		2	Atulasimha ewt al. (2017)
Magneto-Optical (3 separate effects)	1846/1877 /1878	MO Disk drives		2	Tibu et al. (2012)
Mateucci	1847	Magnetoelastics		2	Dimitropoulos and Avaritsiotis (2001)
Magnetoresistance	1856	GMR (automotive)		2	Reig and Cubells-Beltrán (2017)
Wiedemann	1858	Torque sensors		2	Krausa et al., (2008)
Villari	1865	Magnetoelastics		2	Salach et al. (2010)
Lorentz	1879	MEMS	Navigation, Seismics	2	Herrera-May et al. (2017)
Magnetoelectric	1894	Microwave power sensor		2 (room temperature)	Bichurin et al. (2017)
Hall	1899	Cheap and cheerful sensors		2	Salach et al. (2010)
Skin	1903	Proximity sensors		2	Oberhauser (2015)
Sixtus Tonks	1931	Pulse sensors		2, 4	Tibu et al. (2012)
Saturation	**1936**	**Fluxgates**	Mag, EM, MMR	2, 3 good for mag	Janosek (2017)
Precession	*1945*	*Proton magnetometers*	*Mag*	2, 3, 5, 6	Dentith and Mudge, (2014)
Optical Pumping	***1950***	***Total Field (Cs, K, Rb, He)***	*Mag, EM, MMR*	2, 3, 5, 6, 8	Dentith and Mudge, (2014)
Overhauser	*1953*	*Spectroscopy*	*Mag*	2, 3, 5, 6	Dentith and Mudge, (2014)
Josephson	**1962**	**SQUIDs**	EM, Mag grad	4, 7, 8	Schmelz et al., (2011)
Spin Hall Effect	1971	Magnetic memory reading		2	Sinova and Jungwirth (2017)
Atomic resonances	2002	SERF, biomagnetics, Magnetoencephalography		1, 5	Dang et al., (2010)
Nitrogen Vacancy	2012	Fibre-optic, biomagnetics		1, 5	Jensen et al. (2017)
Multipass Cell Atomic	2013			3	Sheng et al. (2013)
Laser threshold	2016			1	Jeske et al. (2016)
Light-Shift Dispersed Mz	2017			3	Schultze et al., 2017

Table 3: Magnetic effects and their useful applications. The right-hand column refers to failure to meet the numbered desirable characteristic from the first column of Table 1. Category 6 (scalar readings) are italicized as they are a "problem" for EM interpretation but an "advantage" in insensitivity to rotation noise.

FARADAY EFFECT SENSORS

The Faraday effect is enshrined in Maxwell's equations, and in simple terms states that the voltage induced in a conductive loop is directly proportional to the rate of change of magnetic flux through the loop. There is an extensive literature on induction coils in general, of which the most comprehensive in my opinion is the review by Dehmel (1989), with a more recent review by Tahiro (2017).

In geophysics, some historic multi-turn EM sensors were designed with mumetal cores (e.g. the airborne Input sensor), some with ferrite cores (e.g. UTEM 3) and some with air cores (e.g. Geonics, Sirotem ground sensors). More recently nano-engineered, ferromagnetic, metallic ribbon materials such as Metglas have provided linear amplitude characteristics plus permitted composite cores to withstand much stronger magnetic fields before saturating, so cored sensors have become lighter and thinner than earlier implementations. Further, ferrite was subject to temperature effects if even slightly fractured in say a drop, so the new ferromagnetic cores are more robust as well.

Good air cored sensors that approach our sensitivity goal of sub 0.1 pT are very large and heavy, so we will analyse only ferromagnetic cored sensors in this review. There are three established electronic options to convert changing magnetic field measurements to voltages, these being 1) Voltage Amplifier, 2) Current Amplifier, and 3) Negative Feedback arrangements (Dehmel, 1989). A simplified summary circuit (Figure 1) shows the key features for each electronic option that are of relevance in predicting sensor noise.

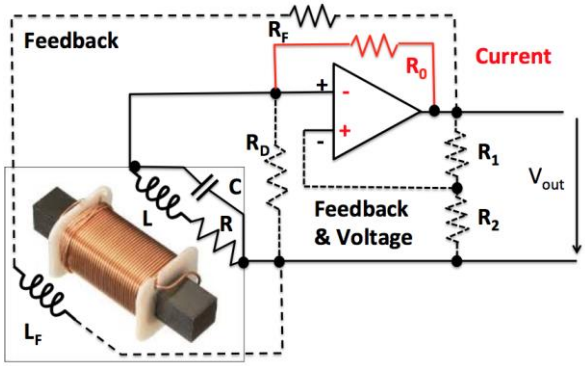

Figure 1: Schematic layout of a ferromagnetic core sensor. Black lines are common to electrical connections of the operational amplifier to the sensor windings in the three electronic schemes. Dashed lines show wiring for the Voltage and / or Feedback arrangements. The red branch is required for the Current amplifier, which also uses the inverting (-) input of the Operational Amplifier.

The sensor hardware will consist of a number of windings on the ferromagnetic core (Figure 1), which can be characterised as having an inductance L and a resistance R in series, with parallel stray capacitance C. To minimize C, important to keep the high frequency characteristics of the coil uniform, it is usual to have multiple coil segments on the core rather than using continuous winding. Voltage sensors require that the high frequency resonance be damped with resistor R_D. For stability, (Dehmel, 1989), this damping resistor needs to be matched to the coil characteristics. The thermal (Johnson) noise from the resistance of the coil itself is small (Figure 2) in all cases for realistic number of turns and size of coil wire. The decrease in coil noise amplitude with frequency is due to the effect of the inductor L in series.

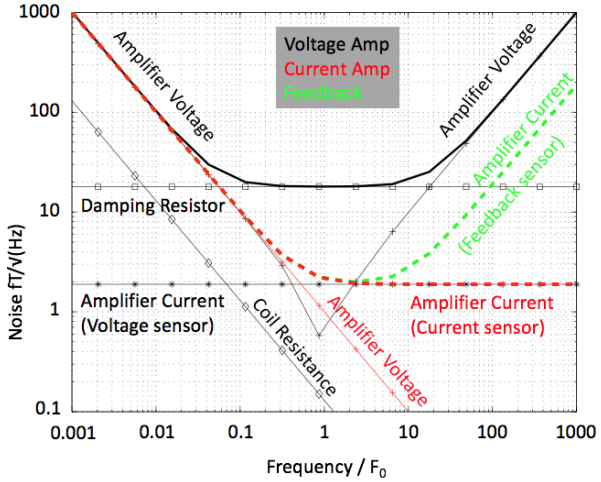

Figure 2: Simulated noise in units of magnetic field for an amplified sensor for the three alternative electronic configurations using the mathematical formulations of Dehmel (1989) and Tahiro (2017). The simulation used typical winding resistance of 100 Ω for a 7-15 mm diameter sensor with 4000 turns of 0.31 mm solid copper wire, and ignored stray capacitance effects. Heavy Red, black and green lines and labels correspond to the current, voltage and feedback arrangements respectively, with the resistance and amplifier noise contributions shown separately. The ideal amplifier had frequency-independent current noise of 10 fA//√Hz and voltage noise 10 pV//√Hz.

Not shown in Figure 2 are the effects of stray capacitance and Barkhausen noise. Because current sensor and feedback geometries keep the core at a constant magnetic field, Barkhausen effects in the core are much less significant sources of noise than in the voltage sensor arrangement.

Any commercial operational amplifier (opamp) will have both current and voltage noise characteristics defined and measured at the input. Choice of an opamp for a low-noise sensor requires analysis of the relative contributions of current and voltage noise in the chosen circuit. For simplicity of explanation, I have made the reasonable approximation that opamp noise is frequency-independent in the bandwidth of interest.

Amplifier voltage noise is the dominant factor at low frequencies, and similar for all of voltage, current, and feedback arrangements. At intermediate frequencies, the noise from the damping resistor dominates the voltage amplifier response. While the feedback circuit uses a damping resistor (Fig 1), it can be set at a much

smaller value of resistance than that required for a voltage amplifier, and so does not contribute significantly to the overall noise in the mid-frequency feedback case.

The opamp current noise is the limiting factor at high frequencies in the current amplifier arrangement, and this noise contribution in the ideal case remains flat over the whole bandwidth as seen in Figure 2. At even higher frequencies, the winding stray capacitance causes some instabilities beyond the range of the plot. In the case of the feedback amplifier, current noise is amplified at high frequencies (green curve in Figure 2). Noise is not the only consideration in sensor choice: dB/dt sensors have a response that increases linearly with frequency. Figure 3 plots signal/noise ratios for the three induction sensors considered.

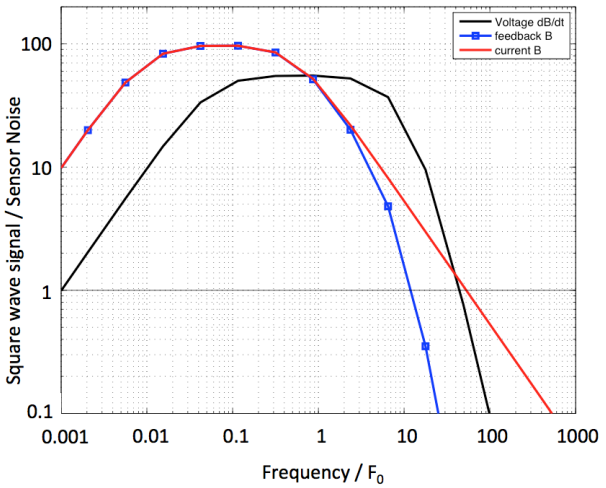

Figure 3: Simulated signal/noise ratios shown in principle for the electronic implementations of induction sensors with frequency independent amplifier noise. Voltage sensors are best at high frequency, with current sensors having a slightly wider useful bandwidth than feedback sensors.

Practical comparisons of EM sensors

Figure 4 presents a comparison of noise levels from specifications (Fluxgate) and shielded chamber measurements (ARMIT and low temperature SQUID). The estimates have been corrected for shielded chamber intrinsic noise. Plotted on the same scale are examples of measured background noise (from natural ionospheric sources, extracted from Chwala et al., 2013). In summer, noise exceeds ARMIT internal noise, so there is no practical advantage in using a SQUID unless a reference is used to help cancel correlated noise. The figure plots the results of using a local reference to reduce natural noise (Chwala et al., 2013) applied to the winter data shown. Local referencing clearly improves the achieved noise levels at low frequencies. However, local referencing has extreme difficulties in the vicinity of powerful transmitters used as sources. Remote referencing on the other hand has 2 issues: the further a reference, the more likely the cultural noise is different and, more than one remote reference is needed in order to correct for timing differences related to the direction of propagation of sferic noise. Referencing, local or remote, has not been applied in routine mineral exploration surveying to my knowledge.

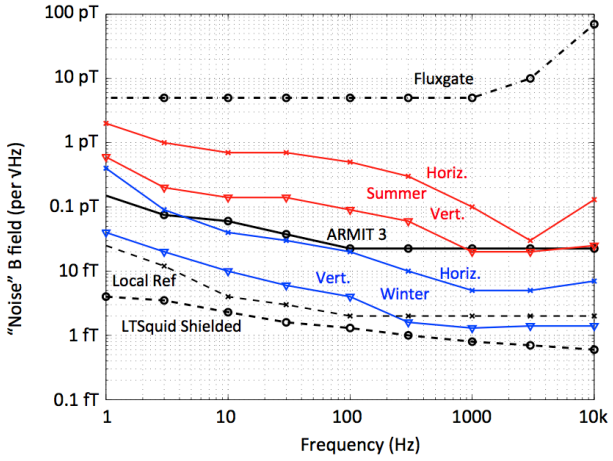

Figure 4: Shielded Chamber internal noise levels (black curves) for Fluxgate, ARMIT 3 and Low temperature SQUID (Chwala et al., 2013) sensors compared with example "natural" noise levels which depend on season and component. The dashed black curve shows that a local reference may help to reduce correlated natural field noise.

Induction magnetometers such as ARMIT have high-pass characteristics (Dehmel, 1989). With the use of high susceptibility, high saturation, linear cores, coupled with electronic signal conditioning, the corner frequency of ARMIT 3 is less than 0.1 Hz. Below 0.1 Hz, signal/noise levels decrease as $1/f^2$ compared to 1/f for SQUIDs, but this frequency range is well below the range of interest in mineral exploration EM. Details of the correction procedure in post-processing of acquired ARMIT data is given in Macnae (2015).

As well as noise, bandwidth at high frequencies is a very important factor in comparing sensors for use in a versatile time-domain system. A sensor with low-pass characteristics is generally unable to obtain the early time data needed for geological mapping of the near-surface.

Figure 5 presents off-time decays measured in the air for an AEM system operating at 25 Hz base frequency. The three components of an ARMIT inductive magnetometer sensor show the "true" secondary field decay with a time constant of less than 1 ms. The airborne ARMIT sensors have a corner frequency of 7 Hz rather than the 0.1 Hz of ARMIT 3, but have similar noise levels above 10 Hz. Setting the high-pass corner at 7 Hz allows signals with frequency content above this corner to be well measured, while rotation noise below the corner is heavily attenuated making for easier corrections.

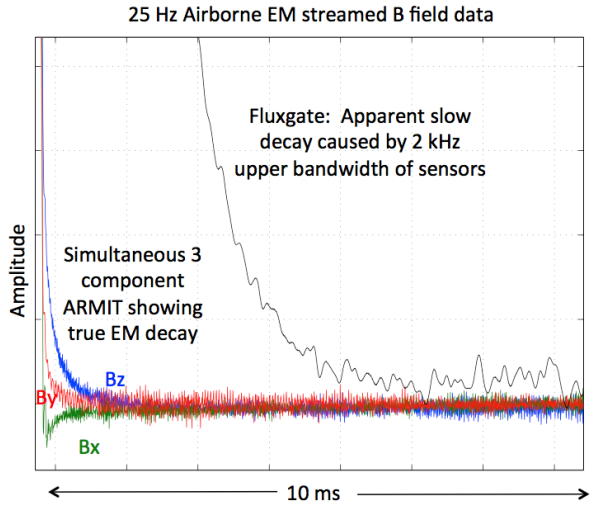

Figure 5: Comparative decays measured by an airborne system immediately following a step-turnoff in current. Unwanted high frequency VLF signals from transmitters > 4000 km away are evident in the three B field decays.

The TFM100G2 (Billingsley Aerospace and Defence) fluxgate data also plotted on Figure 5 on the other hand are a) noisier and b) show an apparent decay of much longer time constant. This apparent slow decay is just the effect of a limited high-frequency bandwidth of 2 kHz as described in Macnae (2015). Lower noise fluxgates are available than those used here (Bazinet, 2014), but they have a lower bandwidth of 300 Hz compared to the 2 kHz of the TFM100G2, and would have an even slower transition after the transmitter switches off, by a factor of about 7.

To assess differences in the field of an ARMIT and a HT SQUID sensor I will analyse one set of data collected in January, 2017 in summer conditions. Figures 6 and 7 present example time series from an audio frequency magnetotelluric (AMT) survey in Western Australia, using an ARMIT 2 sensor as a remote (25.8 km) reference for magnetotelluric sounding combining data from a HT SQUID with measured E fields. ARMIT 2 is somewhat noisier than ARMIT 3 at frequencies below 10 Hz.

Figure 6 shows 4 ms of synchronised data with a large sferic that is very well correlated between the B field sensors. At this scale, sensor noise levels are orders of magnitude below the sferic signal. This sferic, while signal for the AMT survey, would be noise in any controlled source EM data acquisition. Figure 7 shows intermediate frequency "noise" signals of a few hundred pT attributed to communication and electrical systems associated with mining activities 10 or more km away from the survey sites.

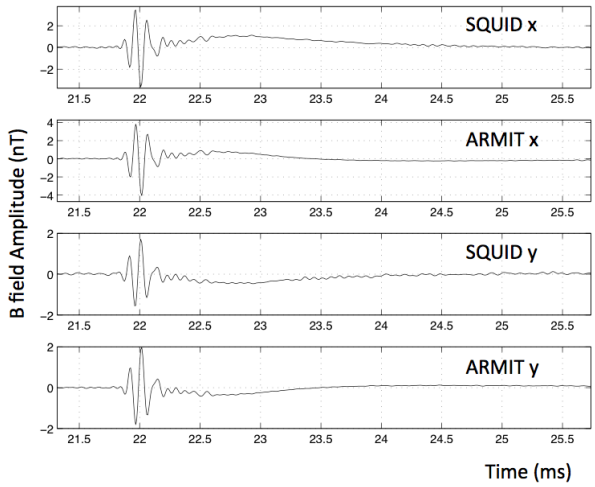

Figure 6: Example of a well-correlated, large sferic in local HT SQUID and synchronised 25.8 km remote ARMIT 2 stations.

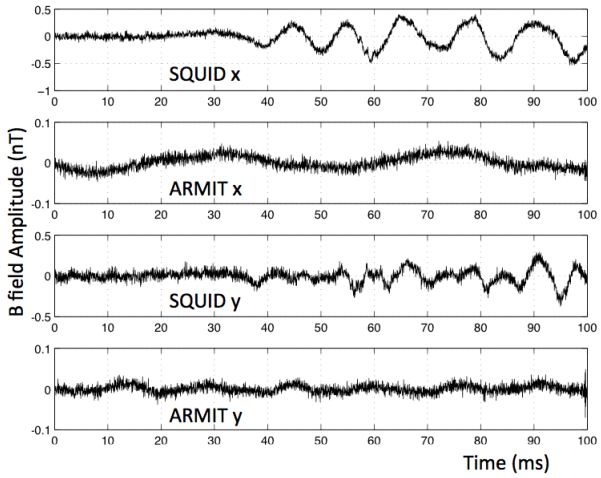

Figure 7: Example 100 ms of synchronised HT SQUID and ARMIT 2 data showing fairly "typical" uncorrelated low-frequency 20 to 200 Hz noise that is likely to be of cultural origin (the local and remote sites were each ~10 km from a number of operating mines). The high-frequency "hash" is VLF from submarine communications and other high-frequency unwanted signals.

Because of the differences seen in Figure 7 between local and remote sites, the value of "remote referencing" to the AMT processing was very limited at these frequencies. Cultural signals below 1 kHz in this environment in the remote Goldfields of Western Australia dominate sensor internal noise. I strongly suspect that processing of controlled source EM data would not be aided by the remote reference data in this and any environment where cultural signals vary widely.

So, in this West Australian survey, both sferic and cultural signals far exceed sensor noise. Different conclusions might well be reached in remote arctic environments in winter conditions with no sferic activity within many thousand km.

Figure 8 shows a spectrum of the frequency content of 500 seconds of the B field data from synchronised HT SQUID and remote reference ARMIT 2 sensors, from which snippets were shown in figures 6 and 7. At first sight, it may seem surprising that the high-temperature SQUID noise is higher than the ARMIT sensor noise.

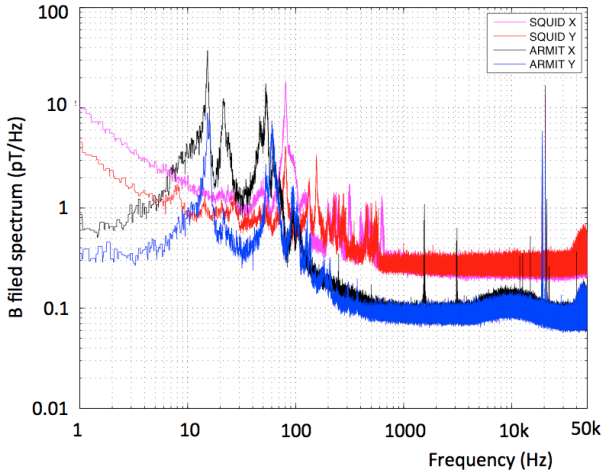

Figure 8. Spectral plot of ARMIT 2 and HT SQUID data from an AMT survey using a remote reference in Western Australia.

There are practical issues in controlled source with 24 bit receivers being used to measure sensor noise unless the DAS gain is high enough. On a Smartem24 system at gain 1 for example, 1 bit corresponds to a HT SQUID signal of 0.8 pT. Gains 100 need to be set to detect signals of the order of the HT SQUID low noise level. Gains greater than 1 however often cause signal overload near transmitters or close to powerlines, and are not automatically adjusted by instrumentation or always adjusted by field crews.

The SQUID data above 1 kHz show higher background noise because the data were collected with gain 1 where the baseline of noise is determined by the DAS and not the sensor itself. The significant differences below 500 Hz are the effect of greater low-frequency cultural noise at the SQUID sensor site.

With the specific HT SQUID sensitivity about 680 nT/V, and ARMIT 2 sensitivity about 180 nT/V, the DAS system noise limited SQUID spectral sensitivity at high frequencies to 0.2 pT/√Hz, to the point that the sferic noise "bump" around 10 kHz seen in the ARMIT data was not evident in the HT SQUID data. All sensors do however clearly detect the VLF signals at 19.8 kHz. Spectral noise attributed to distant mining operations in the 10 to 1000 Hz range is clearly different between the two sets of sensors located 25.8 km apart.

To get optimum low noise from a system close to a transmitter, there is no choice but to use "bucking" as implemented in most compact airborne AEM systems, or restrict measurements to the off-time, or apply variable gain through the waveform. Ground systems to date have not used bucking due to logistical difficulties. One conceptual alternative is to increase the number of bits to say 32, but this is enormously challenging because the 32 bit range would extend from say 1 V to 2 kV (impractical for a receiver) or say 10 nV to 20 V (smallest Voltages too small to be accurately measured).

Typical controlled source EM exploration in Western Australia drives more than 100 A into 100 m or 200 m diameter loops. The magnetic field at the centre of these loops often exceeds 1000 nT.

the HT SQUID is restricted to using gain 1 of a Smartem24, with 0.8 pT resolution at the 1 bit level.

With these strong signals, the HT SQUID is restricted to using gain 1 on a Smartem24, with 0.8 pT resolution at the 1 bit level, or 0.08 pT at gain 10. An ARMIT 2 or 3 sensor however, operated at gain 1 has a least significant bit corresponding to a 0.2 pT signal, and if operated at gain 10, a 0.02 pT signal. The ARMIT sensors do however have a DC offset that at times may prevent operation at higher gain unless it is offset.

Practically, a wider choice of data acquisition system gains than available in Smartem24 would allow optimum noise levels when close to strong transmitter signals. The issues of cultural noise will of course remain whatever the system noise or optimum data acquisition system used.

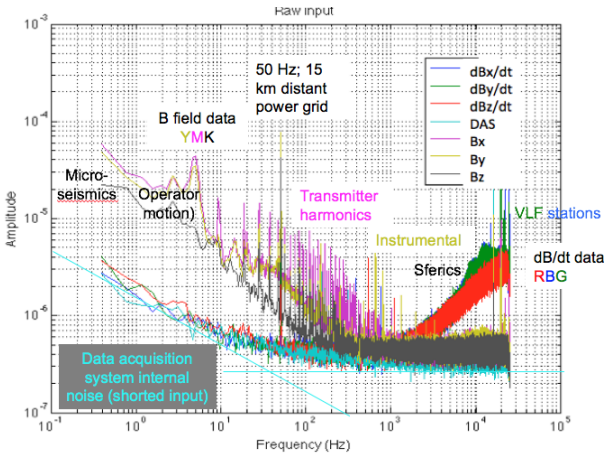

Figure 9: Comparison of simultaneously measured B and dB/dt sensor amplitudes using and ARMIT 2 sensor, with reference DAS shorted input noise in cyan. The data were collected in summer in the field near Heathcote, Victoria. The crossover in sensitivity between B and dB/dt is at 1 kHz. The amplitude is in V//√Hz.

There are a number of HT and LT SQUID systems in operation, each with different specifications. The main point of this paper is that environmental and cultural noise is often the dominant factor affecting the quality of controlled source EM data collection in most conditions, provided that the sensor has a noise level less than 0.1 pT/√Hz. As such, the details of noise specifications of different HT and LT systems are unimportant, as all generally have a flat frequency response in the range of interest, and noise levels well below 0.1 pT/√Hz.

Induction magnetometer choices

An induction magnetometer may be operated as either a B or a dB/dt sensor, as previously described in this article. All ARMIT sensors output both the magnetic field and its time derivative. Figure 9 (Macnae and Kratzer, 2013) is a comparison of B and dB/dt spectra measured by the same coil set. As foreshadowed in Figure 3, it is quite clear is that the dB/dt sensor is better for high-frequency, obtaining signals well above the data acquisition system 1 bit noise, whereas the B sensor is optimum at low frequencies. ARMIT, with both B and dB/dt outputs has obvious advantages in characterizing wideband signals

CONCLUSIONS

Of the 23 or more magnetic effects that have been used for measurement of magnetic fields, sensors based on the Faraday and Josephson effects have proven to be the best for electromagnetic surveys. To be useful, a sensor must have low internal noise and high sensitivity, as well as being linear and capable of operating unscreened in the earth's magnetic field. For sensors with noise levels less than 0.1 pT/√Hz in the EM bandwidth, sferic and rotation rather than internal noise is usually the limiting factor.

All three of induction coils, current and feedback induction magnetometers achieve very low noise levels, provided that their effective area is large and their resistance low, requiring sufficient weight of Cu or Al wire. Feedback and current sensing layouts intrinsically have lower magnetic field noise than coil voltage sensors. Feedback sensors have similar noise levels to current sensors at low frequencies, but like voltage sensors, have increased noise at high frequency when compared to current sensors. In the field, natural noise and the optimum setting of gain in the data acquisition system are controlling factors far more important in data quality than the minimization of internal noise from SQUID and induction magnetometer sensors.

ACKNOWLEDGEMENTS

We thank Thomson Aviation, Monex Geoscope, Newexco Exploration Services and Sandfire Resources for access to field data.

REFERENCES

Atulasimha, J., A. B. Flatau, and J. R. Cullen, 2008, Analysis of the effect of gallium content on the magnetomechanical behavior of single-crystal Fe–Ga alloys using an energy-based model: Smart Materials and Structures, 17, 025027.

Bazinet, R., A. Jacas, G. Confalonieri, and M. Vazquez, 2014, A Low-Noise Fundamental-Mode Orthogonal Fluxgate Magnetometer, IEEE Trans. Magnetics, 50(5), 650103.

Bichurin, M., V. Petrov, R. Petrov, and A Tatarenko, 2017, Magnetoelectric magnetometers, *in* Grosz et al. (eds.), High Sensitivity Magnetometers 127-166, Springer.

Chwala, A., J. Kingman, R. Stolz, M. Schmelz, V. Zakosarenko, S. Linzen, F. Bauer, M Starkloff, M. Meyer and H-G Meyer, 2013, Noise characterization of highly sensitive SQUID magnetometer systems in unshielded environments; Supercond. Sci. Technol. 26, 035017.

Dang, H. B., A. C. Maloof and M. V. Romalis, 2010, Ultrahigh sensitivity magnetic field and magnetization measurements with a atomic magnetometer, Applied Physics Letters 97, 151110.

Dehmel, G., 1989. Magnetic field sensors: induction coil (search coil) sensors: Sensors: A Comprehensive Survey, (5), 205-253.

Dentith M., and S. Mudge, 2014, Geophysics for the mineral exploration geoscientist, Cambridge.

Dimitropoulos, P.D. , and J.N. Avaritsiotis, 2001, A micro-fluxgate sensor based on the Matteucci effect of amorphous magnetic fibers: Sensors and Actuators A: Physical, 94(3), 165–176

Grosz, A., M. J. Haji-Sheikh, and S. C. Mukhopadhyay, (eds.), 2017, High Sensitivity Magnetometers: Smart Sensors, Measurement and Instrumentation 19, Springer.

Herrera-May, a., F. López-Huerta, L. Aguilera-Cortés, 2017, MEMS Lorentz force magnetometers, *in* Grosz et al. (eds.), High Sensitivity Magnetometers 253-277, Springer.

Janosek, J., 2017, Parallel fluxgate magnetometers, *in* Grosz et al. (eds.), High Sensitivity Magnetometers, 41-62, Springer.

Jensen, K., P. Keyayias, and D. Budker, 2017, Magnetometry with nitrogen-vacancy centres in diamond, *in* Grosz et al. (eds.), High Sensitivity Magnetometers, 553-576, Springer.

Jeske, J., J. Cole, and A. Greentree, 2016, Laser threshold magnetometry, New Journal of Physics, 18, 013015.

Krausa, L., M. Malátekb, and M. Dvořákb, 2008, Magnetic field sensor based on asymmetric inverse Wiedemann effect: Sensors and Actuators A: Physical, 142(10), 468–473.

Oberhauser, C., 2010, LDC Sensor Design, Texas Instruments Application Report SNOA930.

Macnae, J., 2015, Correcting EM system bandwidth limitations, ASEG-PESA conference extended abstracts. Available at http://www.publish.csiro.au/ex

Macnae, J., and T. Kratzer, 2013, Joint sensing of B and dB/dt responses, ASEG-PESA conference extended abstracts.

Rieg, C., and M. Cubells-Beltran, 2017, Giant Magnetoresistance (GMR) magnetometers, *in* Grosz et al. (eds.), High Sensitivity Magnetometers, 225-252, Springer.

Salach, J., R. Szewczyk, A. Bienkowski, and P. Frydrych, 2010. Methodology of testing the magnetoelastic characteristics of ring-shaped cores under uniform compressive and tensile stresses. Journal of Electrical Engineering. 61(7), 93.

Schmelz, M., R. Stolz, V. Zakosarenko, T. Schönau, S. Anders, L. Fritzsch, M. Mück and H.-G. Meyer, 2011, Field-stable SQUID magnetometer with sub-fT $Hz^{-1/2}$ resolution based on sub-micrometer cross-type Josephson tunnel junctions, Superconductor Science and Technology, 24, 065009.

Schultze, V., B. Schillig, R Ijesselsteijn, S. Woetzel, and R. Stolz, 2017, An optically pumped magnetometer working in the light-shift dispersed M_z mode. Sensors 2017, 17, 561

Sheng, D., S. Li, N. Dural, and M. Romalis, 2013, Subfemtotesla scalar atomic magnetometry using multipass cells, Physical Review Letters 110, 160802.

Sinova, J., and T. Jungwirth, 2017, Surprises from the spin Hall effect, Physics today, 70, 7, 38-42.

Storm, J.-H., P. Hömmen, D. Drung, and R. Körber, 2017, An ultra-sensitive and wideband magnetometer based on a superconducting quantum interference device; Appl. Phys. Lett. 110, 072603.

Tahiro, K., 2017, Induction coil magnetometers, *in* Grosz et al. (eds.), High Sensitivity Magnetometers, 225-252, Springer.

Tibu, M., M. Losun, and H. Chiriac, 2012, Simultaneous magneto-optical Kerr effect and Sixtus-Tonks method for analyzing the shape of propagating domain walls in ultrathin magnetic wires: Rev. Sci. Instrum., 83(6), 064708. doi: 10.1063/1.4729601.